Hindawi Publishing Corporation
Journal of Nanomaterials
Volume 2016, Article ID 2895850, 5 pages
http://dx.doi.org/10.1155/2016/2895850

Research Article

Preparation of Composite Films of a Conjugated Polymer and C_{60}NWs and Their Photovoltaic Application

Takatsugu Wakahara,[1] Kun'ichi Miyazawa,[1] Osamu Ito,[1] and Nobutaka Tanigaki[2]

[1]*Fullerene Engineering Group, Advanced Materials Processing Unit, Advanced Key Technologies Division, National Institute for Materials Science (NIMS), 1-1 Namiki, Tsukuba, Ibaraki 305-0044, Japan*
[2]*Integrated Functional Materials Group, Inorganic Functional Materials Research Institute, National Institute of Advanced Industrial Science and Technology, 1-18-31 Midorigaoka, Ikeda, Osaka 563-8577, Japan*

Correspondence should be addressed to Takatsugu Wakahara; wakahara.takatsugu@nims.go.jp

Received 6 April 2016; Accepted 22 May 2016

Academic Editor: Guoqing Ning

Composite films of conjugated polymers, such as poly[2-methoxy-5-(3′,7′-dimethyloctyloxy)-1,4-phenylenevinylene] (MDMO-PPV) and poly(3-hexylthiophene) (P3HT), with C_{60} nanowhiskers (C_{60}NWs) were prepared. The photoluminescence originating from the conjugated MDMO-PPV polymers was effectively quenched in the composite film, indicating a strong interaction between the conjugated polymer and C_{60}NWs. The photovoltaic devices were fabricated using C_{60}NW (conjugated polymer) composite films, resulting in a power conversion efficiency of ~0.01% for P3HT with short length thin C_{60}NWs, which is higher than that previously reported for thick C_{60} nanorods. The present study gives new guidance on the selection of the type of C_{60}NWs and the appropriate polymer for new photovoltaic devices.

1. Introduction

Due to their unique physical and chemical properties, fullerenes have tremendous potential as building blocks for new materials [1]. Recently, fullerene-based supramolecular nanoarchitecture, such as nanowhiskers [2], nanotubes [3], nanorods [4], nanowires [5], and nanosheets [6, 7], has attracted special interest because of their unique chemical and physical properties and their possible application in the fields of materials and medical sciences. Their unique properties are a result of the high symmetry of the nanoarchitecture and the presence of novel π-conjugated systems in supramolecular nanoarchitecture. Very recently, high photosensitivity and excellent electron accepting nature of C_{60} nanorods were reported by Saran et al. [8]. They also demonstrated that the photosensitivity of the C_{60} nanorods can be enhanced by organic and inorganic photodoping [8].

Fullerenes form a wide variety of donor-acceptor complexes with different classes of organic and organometallic donors [9]. These complexes possess a wide range of physical properties, including metallic, photoconductive, and unusual magnetic properties. Within this family, we have recently reported the preparation of C_{60}/ferrocene hybrid nanosheets [10, 11] and C_{60}/Co-porphyrin nanosheets [12] by a liquid-liquid interfacial precipitation (LLIP) method. These nanosheets showed very unique optical and charge transport properties.

In various donor molecules, conjugated polymers such as polyphenylenevinylene (PPV) are well known and have been widely studied as photoactive materials in organic thin-film transistors (OTFTs) [13] and organic photovoltaics (OPVs) [14]. To date, various blends of conjugated polymers and fullerene molecules have been reported to fabricate the effective OTFTs and OPVs [15]. In such cases, PCBM (C_{60} ester derivative) soluble in organic solvents was the most effective one; however, after fabricating the blend films, the molecules were present mostly as aggregates forming the chain structure, through which electrons migrate efficiently [16].

We herein report the preparation of composite films of C_{60} nanowhiskers (C_{60}NWs), instead of the C_{60} molecules because the C_{60}NWs are known to exhibit high electron

mobility [17–19]. The observed mobility of well-aligned 1D C_{60} nanocrystals [19] was also much higher than that of PCBM [20]. The C_{60}NWs were then mixed with well-employed conjugated polymers (poly[2-methoxy-5-(3′,7′-dimethyl-octyloxy)-1,4-phenylene-vinylene] (MDMO-PPV) and poly(3-hexylthiophene) (P3HT)). Thus, C_{60}NWs are expected to be efficient new blend components.

The conjugated polymers (MDMO-PPV and P3HT) were employed because these conjugated polymers are well-known photoenergy harvesting polymers with electron donating ability.

In the present study, we found that the photoluminescence originating from MDMO-PPV was effectively quenched in the composite films, indicating a strong interaction between the conjugated polymers and C_{60}NWs. The photovoltaic devices were also fabricated using C_{60}NW (conjugated polymer) composite films; the power conversion efficiency varied with the diameter and length of the C_{60}NWs, in addition to the type of polymer and device structure.

2. Materials and Methods

2.1. Materials. The C_{60}NWs used in this study were prepared by a liquid-liquid interfacial precipitation (LLIP) method in which C_{60}NWs were formed at an interface between the C_{60}-containing benzene and isopropyl alcohol (IPA). In a typical preparation, 4 mL of C_{60}-saturated benzene was placed into a glass bottle in an ice bath. To this solution, 8 mL of IPA was added slowly, and the resulting two-layer mixture was vigorously shaken and subjected to ultrasonication for 1 min. The resulting mixture was stored at 5°C for 24 h to grow C_{60}NWs.

2.2. Optical Measurements. Optical microscope images were observed with an Olympus BX51. UV-Vis-NIR spectra of the films were measured by UV-Vis-NIR spectrometer (V-570, JASCO, Japan) equipped with an integrating sphere in the reflection geometry. Photoluminescence spectra were measured by fluorescence spectroscopy (FP-6600, JASCO, Japan).

2.3. Preparation and Characterization of Photovoltaic Devices. Photovoltaic devices based on C_{60}NWs were prepared as follows. A film of poly(3,4-dioxythiophene) : poly(styrene sulfonate) (PEDOT : PSS) was deposited onto prepatterned ITO electrodes by spin-coating (HC Stark), followed by annealing at 100°C for 1 h. C_{60}NWs film was prepared on the ITO electrodes by casting C_{60}NW solution. The solution of conjugated polymers (5 mg/mL) was spin-coated onto the C_{60}NW film. After annealing at 80°C for 8 h under vacuum, LiF (~0.5 nm) and Al (~100 nm) were deposited under vacuum to completely fabricate the devices; ITO/PEDOT : PSS/C_{60}NWs-polymer/LiF/Al, which contained poly[2-methoxy-5-(3′,7′-dimethyloctyloxy)-1,4-phenylenevinylene] (MDMO-PPV) and poly(3-hexylthiophene) (P3HT), were employed as polymers.

The devices were characterized using Ivium CompactStat (Ivium Technologies) under an AM 1.5 G (1 sun 100 mW/cm^2) illumination from an OTENTO-SUN-III (Bunkoukeiki, Japan) solar simulator after annealing at 150°C for 20 min under Ar atmosphere.

3. Results and Discussion

In 2007, the preparation of nanoporous C_{60}NWs by the LLIP method at the interface between the C_{60}-containing benzene and isopropyl alcohol (IPA) was reported in our group [21]. The formation of pores has been confirmed by the observed higher specific surface area of 376 m^2/g, whereas the specific surface area of pristine C_{60} powder is 20 m^2/g. The fine pores on the wall surface of C_{60}NWs were also observed by TEM [21]. Recently, we used nanoporous C_{60}NWs to prepare C_{60}NWs modified onto glassy carbon (GC) electrodes to study the electrochemical reduction of oxygen, suggesting that nanoporous C_{60}NWs are electrochemically active materials [22]. Therefore, in the present study, we also used these nanoporous C_{60}NWs to prepare C_{60}NW-(MDMO-PPV) composite films.

We prepared the C_{60}NW-MDMO-PPV composite films by casting a cyclohexanone solution of MDMO-PPV onto C_{60}NW films on a glass plate. Figure 1 shows the optical microscope images of the (a) C_{60}NWs and (b) C_{60}NW-MDMO-PPV composite films. The photographs of three films are also shown in Figure 1.

The C_{60}NW film in Figure 1(a) was prepared by casting a benzene/IPA solution of C_{60}NWs onto a glass plate, in which most of the C_{60}NWs had diameters less than 100 nm and some C_{60}NWs had larger diameters (~1 μm). The lengths of C_{60}NWs ranged from 100 μm to 1000 μm. The representative image in Figure 1(b) shows that the one-dimensional morphology of C_{60}NWs was retained even after the formation of the composite film and that the larger diameters of C_{60}NW-MDMO-PPV composite became prominent and hid smaller ones under the polymer film. The interface between C_{60}NWs and MDMO-PPV was not as clear, indicating that C_{60}NWs and MDMO-PPV fused together at the interface. This can be related to the increase in diameter of the C_{60}NW-MDMO-PPV composite. Furthermore, fattening of C_{60}NWs would be expected with polymer wear, and advances in the aggregation of the C_{60}NWs with the cyclohexanone solution containing MDMO-PPV would also be anticipated.

Figures 1(c)–1(e) show photographs of the C_{60}NWs, MDMO-PPV, and the C_{60}NW-MDMO-PPV composite films on glass plates. Although the C_{60} powders appeared black in color, the C_{60}NW thin film had a yellow ocher color on the glass plate, as shown in Figure 1(c). The orange color of the C_{60}NW-MDMO-PPV composite film became darker compared to the bright reddish orange color of the MDMO-PPV film, supporting the formation of the C_{60}NW-MDMO-PPV composite.

Figure 2 shows the UV-Vis-NIR spectra of the C_{60}NWs, MDMO-PPV, and the C_{60}NW-MDMO-PPV composite film. The UV-Vis-NIR spectrum of the C_{60}NW film contained the main bands at 307 and 440 nm with broad weak bands at 620 nm. This spectrum corresponds to the solution absorption spectrum of C_{60} with broadening due to weak interactions among the C_{60} molecules in the C_{60}NWs. The diffuse reflectance spectrum of MDMO-PPV contained peaks at 420 and 580 nm with a sharp cut-off at 600 nm. The diffuse reflectance spectrum of the C_{60}NW-MDMO-PPV composite film clearly showed a superposition of the C_{60}NWs and

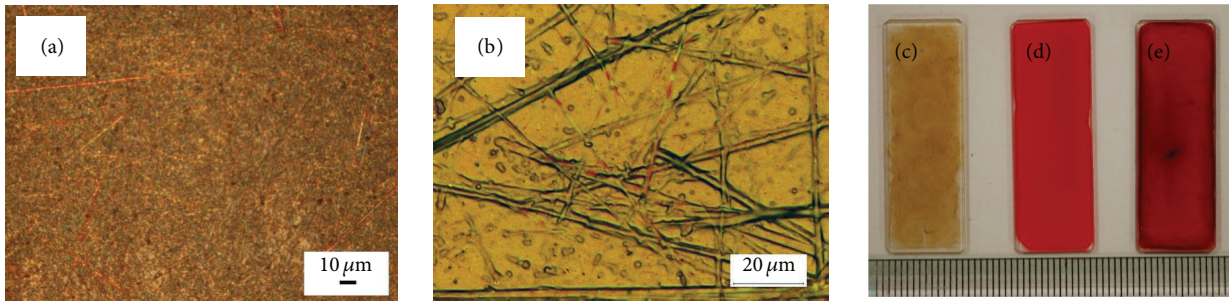

Figure 1: Optical microscope images of (a) C_{60}NWs and (b) C_{60}NW-MDMO-PPV composite films. Photographs of composite films on glass plates (38 × 13 mm): (c) C_{60}NWs, (d) MDMO-PPV, and (e) C_{60}NW-MDMO-PPV.

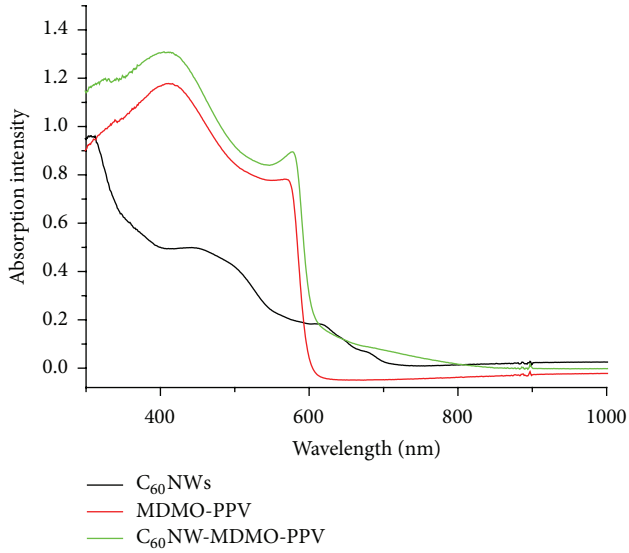

Figure 2: UV-Vis-NIR spectra of MDMO-PPV (red), C_{60}NWs (black), and C_{60}NW-MDMO-PPV composite films (green).

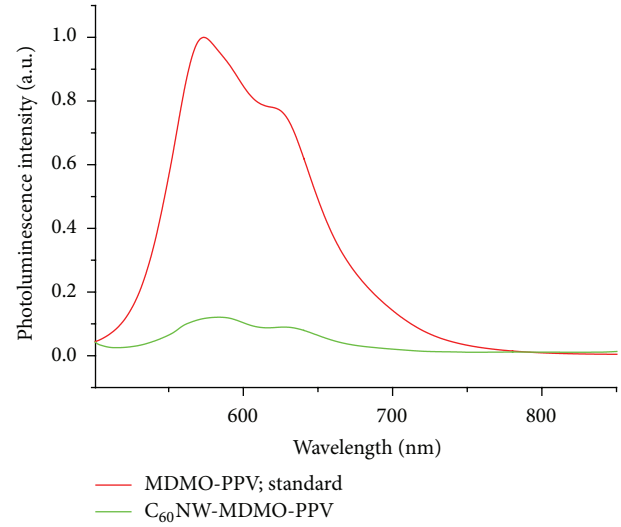

Figure 3: Photoluminescence spectra of MDMO-PPV (red) and the composite film of C_{60}NW-MDMO-PPV (green). Excitation wavelength = 485 nm.

MDMO-PPV films. Near 700 nm, a new broad absorption tail appeared, suggesting a weak interaction between the components. From Figure 1(b), because the verges of the C_{60}NWs were clearly observed at micrometer optical resolution, appreciable adsorption of the MDMO-PPV occurred on the C_{60}NWs, which may be related to this absorption tail.

Figure 3 shows the photoluminescence spectra of the composite film of C_{60}NWs and MDMO-PPV. The photoluminescence originating from MDMO-PPV decreased to 10% in the composite film, suggesting an appreciable interaction between MDMO-PPV and the C_{60}NWs in the excited state; the ground state interaction may also contribute to the emission quenching, as suggested by the absorption tailing near 700 nm in Figure 2. From Figure 1(b), the verges of the C_{60}NWs are clearly shown at micrometer optical resolution; appreciable adsorption of MDMO-PPV on the C_{60}NWs could also be a source of the fluorescence quenching.

Until now, the various blends of conjugated polymers such as PPV and P3HT have been used as active materials as a pair of fullerenes in the organic photovoltaics (OPVs), imparting high solar energy conversion. This inspires us to fabricate new OPVs using the C_{60}NW-polymer composite films as active materials. Figure 4 shows the current-voltage characteristics of a device made from the C_{60}NW-MDMO-PPV composite film. The device structure consisted of ITO/PEDOT : PSS/C_{60}NWs-MDMO-PPV/LiF/Al. The short-circuit current (I_{SC}) and open-circuit voltage (V_{OC}) under AM 1.5 G 1 sun illumination were 0.20 mA/cm^2 and 0.73 V, respectively; the fill factor (FF) was 0.23, and the power conversion efficiency (PCE) was 0.033%, as listed in Table 1.

In polymer-PCBM OPVs, the carrier mobility is higher in P3HT-PCBM blends compared to that in MDMO-PPV-PCBM [23]. Therefore, we fabricated OPVs using P3HT as a conjugated polymer to construct the device structure of ITO/PEDOT : PSS/C_{60}NWs-P3HT/LiF/Al. The C_{60}NW-P3HT composite film was prepared by spin-coating a toluene solution of P3HT onto the C_{60}NW films. The optical microscope image and diffuse reflectance spectrum of the C_{60}NW-P3HT composite film are shown in Figures S1 and S2 in Supplementary Material available online at http://dx.doi.org/10.1155/2016/2895850. The properties of the

Table 1: Properties of C_{60}NW (C_{60} nanorod) OPVs.

	I_{SC}/mA	V_{OC}/V	FF	PEC/%	Source
ITO/PEDOT : PSS/C_{60}NWs-MDMO-PPV/LiF/Al	0.20	0.73	0.23	0.033	This work
ITO/PEDOT : PSS/C_{60}NWs-P3HT/LiF/Al	0.56	0.36	0.38	0.075	This work
ITO/PEDOT : PSS/P3HT/s-C_{60}NWs-P3HT/LiF/Al	0.46	0.51	0.42	0.097	This work
n-Si/P3OT-C_{60} nanorod/Au	0.0098	0.155	0.1485	0.0002	[24]
ITO/PEDOT : PSS/P3HT-C_{60} nanorods/Al	0.091	NA	NA	NA	[25]

I_{SC}: short-circuit current; V_{OC}: open-circuit voltage; FF: fill factor; and PCE: power conversion efficiency. Under AM 1.5 G 1 sun illumination. NA: not available.

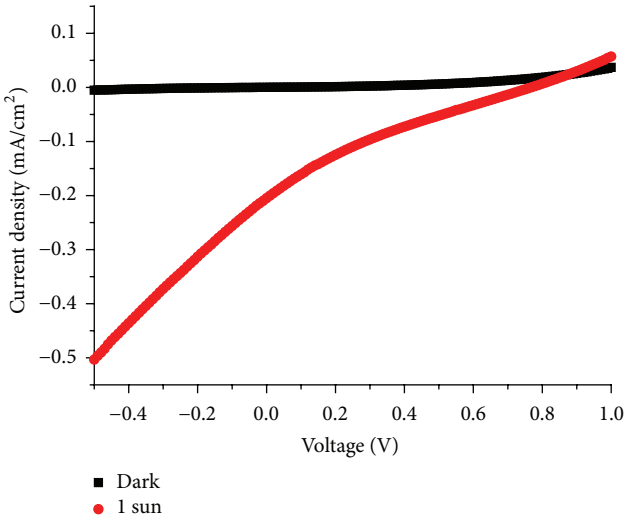

Figure 4: Current-voltage characteristics of the device with the C_{60}NW-MDMO-PPV film (ITO/PEDOT : PSS/C_{60}NWs-MDMO-PPV/LiF/Al) under AM 1.5 G (1 sun 100 mW/cm^2) illumination from OTENTO-SUN-III (Bunkoukeiki) solar simulator.

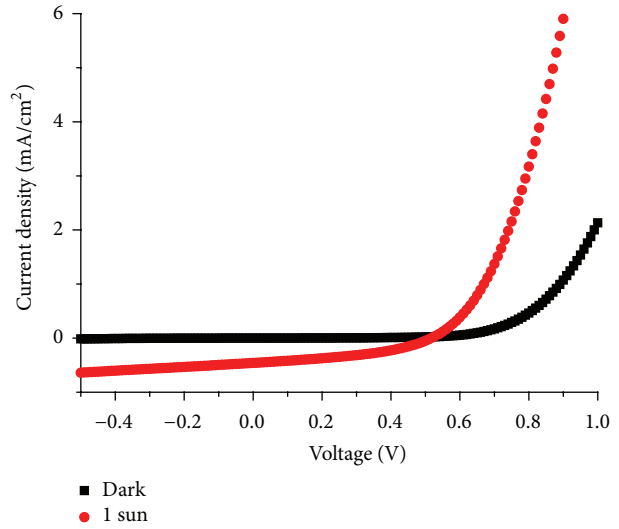

Figure 5: Current-voltage characteristics of the device with ITO/PEDOT : PSS/P3HT/s-C_{60}NW-P3HT/LiF/Al film.

C_{60}NW-P3HT OPVs are also summarized in Table 1. Compared to MDMO-PPV as a partner of C_{60}NWs, the OPV device performance was improved by P3HT (PCE = 0.075%).

We also fabricated OPVs employing short-C_{60}NWs (s-C_{60}NWs) prepared by sonication of C_{60}NW solutions. The device structure consisted of ITO/PEDOT : PSS/P3HT/s-C_{60}NWs-P3HT/LiF/Al. In this device, s-C_{60}NWs were used to prepare thinner C_{60}NW films, and we also inserted a new P3HT layer to inhibit contact between the s-C_{60}NWs and ITO. As shown in Figure 5, I_{SC} and V_{OC} under AM 1.5 G 1 sun illumination were 0.46 mA/cm^2 and 0.51 V, respectively, and the PCE increased up to 0.097%. There are two previous reports on the fabrication of OPVs using C_{60} nanorods with larger diameters (500–1000 nm [24] and 215 nm [25]) than our C_{60}NWs (~100 nm). Compared to these reported values, we demonstrated an improvement in the device performance. Furthermore, our C_{60}NWs prepared with benzene and an IPA interface were porous (our C_{60}NWs have a much higher specific surface area than either pristine C_{60} powder or other 1D C_{60} nanocrystals [21, 26, 27]), which may be beneficial for stronger interactions between the C_{60}NWs and conjugated polymers. Our results indicate that the physical properties (high surface area and small diameter) of C_{60}NWs are important for C_{60}NW OPVs.

4. Conclusion

We prepared composite films of conjugated polymers, MDMO-PPV and P3HT, with C_{60}NWs prepared from benzene and an IPA interface with the LIIP method. The photoluminescence originating from the polymers (e.g., MDMO-PPV) was effectively quenched in the composite films, indicating strong interactions between MDMO-PPV and the C_{60}NWs. The applicability of polymer-C_{60}NW composite films in photovoltaic devices was also successfully demonstrated. The physical properties (high surface area and small diameter) of the C_{60}NWs played an important role in improving the OPVs. In addition, selection of conjugated polymers as a pair of C_{60}NWs is also crucial.

Competing Interests

The authors declare that there is no conflict of interests regarding the publication of this paper.

Acknowledgments

A part of this research was supported by a Grant-in-Aid for Scientific Research from the Ministry of Education and Culture, Sports, Science and Technology of Japan.

References

[1] M. Prato, "[60]Fullerene chemistry for materials science applications," *Journal of Materials Chemistry*, vol. 7, no. 7, pp. 1097–1109, 1997.

[2] K. Miyazawa, Y. Kuwasaki, A. Obayashi, and M. Kuwabara, "C_{60} nanowhiskers formed by the liquid-liquid interfacial precipitation method," *Journal of Materials Research*, vol. 17, no. 1, pp. 83–88, 2002.

[3] K. Miyazawa, J. Minato, M. Fujino, and T. Suga, "Structural investigation of heat-treated fullerene nanotubes and nanowhiskers," *Diamond and Related Materials*, vol. 15, no. 4–8, pp. 1143–1146, 2006.

[4] Y. Jin, R. J. Curry, J. Sloan et al., "Structural and optoelectronic properties of C_{60} rods obtained via a rapid synthesis route," *Journal of Materials Chemistry*, vol. 16, no. 37, pp. 3715–3720, 2006.

[5] J. Geng, W. Zhou, P. Skelton et al., "Crystal structure and growth mechanism of unusually long fullerene (C-60) nanowires," *Journal of the American Chemical Society*, vol. 130, no. 8, pp. 2527–2534, 2008.

[6] M. Sathish and K. Miyazawa, "Size-tunable hexagonal fullerene (C_{60}) nanosheets at the liquid-liquid interface," *Journal of the American Chemical Society*, vol. 129, no. 45, pp. 13816–13817, 2007.

[7] T. Wakahara, Y. Nemoto, M. Xu, K.-I. Miyazawa, and D. Fujita, "Preparation of endohedral metallofullerene nanowhiskers and nanosheets," *Carbon*, vol. 48, no. 12, pp. 3359–3363, 2010.

[8] R. Saran, V. Stolojan, and R. J. Curry, "Ultrahigh performance C_{60} nanorod large area flexible photoconductor devices via ultralow organic and inorganic photodoping," *Scientific Reports*, vol. 4, article 5041, 2014.

[9] D. V. Konarev, R. N. Lyubovskaya, N. V. Drichko et al., "Donor-acceptor complexes of fullerene C60 with organic and organometallic donors?" *Journal of Materials Chemistry*, vol. 10, no. 4, pp. 803–818, 2000.

[10] T. Wakahara, M. Sathish, K. I. Miyazawa et al., "Preparation and optical properties of fullerene/ferrocene hybrid hexagonal nanosheets and large-scale production of fullerene hexagonal nanosheets," *Journal of the American Chemical Society*, vol. 131, no. 29, pp. 9940–9944, 2009.

[11] T. Wakahara, M. Sathish, K. Mizayawa, and T. Sasaki, "Organic-metal-doped fullerene nanowhiskers," *Nano*, vol. 3, no. 5, pp. 351–354, 2008.

[12] T. Wakahara, P. D'Angelo, K. Miyazawa et al., "Fullerene/cobalt porphyrin hybrid nanosheets with ambipolar charge transporting characteristics," *Journal of the American Chemical Society*, vol. 134, no. 17, pp. 7204–7206, 2012.

[13] R. J. O. M. Hoofman, M. P. de Haas, L. D. A. Slebbeles, and J. M. Warman, "Highly mobile electrons and holes on isolated chains of the semiconducting polymer poly(phenylene vinylene)," *Nature*, vol. 392, no. 6671, pp. 54–56, 1998.

[14] K. Masuda, Y. Ikeda, M. Ogawa, H. Benten, H. Ohkita, and S. Ito, "Exciton generation and diffusion in multilayered organic solar cells designed by layer-by-layer assembly of poly(p-phenylenevinylene)," *ACS Applied Materials and Interfaces*, vol. 2, no. 1, pp. 236–245, 2010.

[15] G. Dennler, M. C. Scharber, and C. J. Brabec, "Polymer-fullerene bulk-heterojunction solar cells," *Advanced Materials*, vol. 21, no. 13, pp. 1323–1338, 2009.

[16] M. Campoy-Quiles, T. Ferenczi, T. Agostinelli et al., "Morphology evolution via self-organization and lateral and vertical diffusion in polymer: fullerene solar cell blends," *Nature Materials*, vol. 7, no. 2, pp. 158–164, 2008.

[17] K. Ogawa, T. Kato, A. Ikegami et al., "Electrical properties of field-effect transistors based on C-60 nanowhiskers," *Applied Physics Letters*, vol. 88, no. 11, Article ID 112109, 2006.

[18] T. Doi, K. Koyama, Y. Chiba et al., "Electron transport properties in photo and supersonic wave irradiated C_{60} fullerene nanowhisker field-effect transistors," *Japanese Journal of Applied Physics*, vol. 49, no. 4, Article ID 04DN12, 2010.

[19] H. Li, B. C.-K. Tee, J. J. Cha et al., "High-mobility field-effect transistors from large-area solution-grown aligned C_{60} single crystals," *Journal of the American Chemical Society*, vol. 134, no. 5, pp. 2760–2765, 2012.

[20] P. H. Wöbkenberg, D. D. C. Bradley, D. Kronholm et al., "High mobility n-channel organic field-effect transistors based on soluble C-60 and C-70 fullerene derivatives," *Synthetic Metals*, vol. 158, no. 11, pp. 468–472, 2008.

[21] M. Sathish, K. Miyazawa, and T. Sasaki, "Nanoporous fullerene nanowhiskers," *Chemistry of Materials*, vol. 19, no. 10, pp. 2398–2400, 2007.

[22] T. Wakahara, M. Sathish, K. Miyazawa, and O. Ito, "Electrochemical characterization of catalytic activities of C_{60} nanowhiskers to oxygen reduction in aqueous solution," *Fullerenes Nanotubes and Carbon Nanostructures*, vol. 23, no. 6, pp. 509–512, 2015.

[23] A. Pivrikas, N. S. Sariciftci, G. Juška, and R. Österbacka, "A review of charge transport and recombination in polymer/fullerene organic solar cells," *Progress in Photovoltaics: Research and Applications*, vol. 15, no. 8, pp. 677–696, 2007.

[24] P. R. Somani, S. P. Somani, and M. Umeno, "Toward organic thick film solar cells: three dimensional bulk heterojunction organic thick film solar cell using fullerene single crystal nanorods," *Applied Physics Letters*, vol. 91, no. 17, Article ID 173503, 2007.

[25] R. G. Shrestha, L. K. Shrestha, A. H. Khan, G. S. Kumar, S. Acharya, and K. Ariga, "Demonstration of ultrarapid interfacial formation of 1D fullerene nanorods with photovoltaic properties," *ACS Applied Materials and Interfaces*, vol. 6, no. 17, pp. 15597–15603, 2014.

[26] C. L. Ringor and K. Miyazawa, "Synthesis of C_{60} nanotubes by liquid-liquid interfacial precipitation method: influence of solvent ratio, growth temperature, and light illumination," *Diamond and Related Materials*, vol. 17, no. 4-5, pp. 529–534, 2008.

[27] L. K. Shrestha, R. G. Shrestha, Y. Yamauchi et al., "Nanoporous carbon tubes from fullerene crystals as the π-electron carbon source," *Angewandte Chemie—International Edition*, vol. 54, no. 3, pp. 951–955, 2015.